Characterizing Pilot Anodes Made with CTP and Bio-Pitch using µCT

Stein Rørvik[1], Gøril Jahrsengene[2], Asem Hussein[3] and Houshang Alamdari[4]
1. Research Scientist
2. Research Scientist
SINTEF Industry, Trondheim, Norway
3. Research Scientist, Elkem Carbon Solutions, Kristiansand, Norway
Previously: PhD Candidate, Aluminum Research Centre–REGAL, Mining, Material, and Metallurgy Engineering Department, Université Laval, Québec, Canada
4. Professor of Aluminum Research Centre–REGAL, Mining, Materials, and Metallurgy Engineering Department, Université Laval, Québec, Canada
Corresponding author: goril.jahrsengene@sintef.no

Abstract

Replacing the fossil-based binder phase in pre-baked anodes with materials originating from wood pyrolysis products is suggested as a CO_2-neutral alternative to the currently used coal tar pitch (CTP). Recent work shows that bio-pitches (BPs) upgraded from bio-oils (or similar pyrolysis products) have good wetting towards calcined petroleum coke (CPC), and despite the relatively low coking value and the high reactivity of the bio-pitches, pilot-anodes with physical and electrochemical properties comparable to those made from CTP have been produced. The pilot anodes with bio-pitch have a higher shrinkage upon baking than anodes made from CTP, presumed to be due to the higher baking loss and better wetting between the coke and the BP. In this study the anode structure, including this shrinkage, is characterized using micro X-ray computed tomography (µCT). One pilot anode made from BP and one pilot anode made from CTP were scanned using µCT, baked, and then re-scanned using µCT after baking. The pre- and post-baking datasets are aligned in the image analysis software, allowing a direct comparison of the pre- and post-baking state.

Keywords: CO_2-neutral aluminium production, Bio-pitch, Pilot anodes, µCT.

1. Introduction

Calcined petroleum coke (CPC), recycled anode butts and coal tar pitch (CTP) are traditionally used in pre-baked anodes for aluminium production. To potentially reduce the carbon footprint in aluminium production, the fossil-based materials are suggested to be replaced by biocarbon options. Replacing the CPC with biocarbon seems difficult, and current research shows that only small amounts of biocarbon filler can be introduced in the anodes [1-3]. Replacing the CTP appears to be a better option to produce greener aluminium through biocarbon addition and may additionally reduce the toxic polycyclic aromatic hydrocarbon (PAH) emissions during the baking process.

Bio-pitch (BP) can be produced from bio-oils or other liquid products from pyrolysis of biomass (woods) [4]. Important parameters to evaluate and compare to those of CTP include coking value (CV), softening point (SP) and wetting behaviour when interacting with CTP. Typical BPs have lower CV and SP than traditional materials, but these properties can be somewhat controlled by changing the production parameters (temperature, heating rate, holding time and, pressure, in the case of vacuum pyrolysis) [5]. Lower SP may result in less energy consumption during mixing of anode paste, but low CV is traditionally associated with a more porous anode. Additionally, BPs have been found to not graphitize well, retaining an amorphous structure. An amorphous carbon typically exhibits higher electrical resistivity in the binder phase [6].

Despite the initial beliefs that anodes made from BPs with low CV will result in poor anodes, pilot anodes with CTP and BP have been produced with comparable physical [6] and electrochemical [7] properties. This has been theorized to be caused by the superior wetting properties of the BP towards CPC, compared to CTP. Studies [5] have shown good wetting behaviour during mixing, and a significantly larger shrink is observed for pilot anodes made from BPs (5 % vs 2.5 % in [6]). In theory, this may result in shorter distance between the coke particles, which will mitigate the larger loss of binder phase upon baking and the lower graphitization degree of this material.

In this study, the imaging technique of micro X-ray computed tomography (µCT) has been used to characterize several pilot anodes made from CTP and BP to get a better understanding of the wetting between binder and filler during production of green anodes, of possible shrinkage mechanisms during baking, and their effect on general quality of pilot anodes. The main advantage of µCT imaging is that it is non-destructive and gives data for the full sample volume. This allows for comparison of the same sample before and after some treatment; in this case baking at 1100 ºC.

2. Experimental

2.1 Pilot Anodes

For this study, BP was produced by the same procedure as described in [6], using atmospheric pressure, a heating rate of 0.5 °C/min up to 180 °C, and a soaking time of 1 hour. This treatment on the same bio-oil has previously been showed to result in a bio-pitch with a SP in the range of 85-90 °C and a CV of almost 35 %. Two series of pilot anodes were produced for the present study, using either the described BP or a CTP with a Mettler SP of 100 °C and CV of 62 %. Calcined petroleum coke with specific fractions (see more details in [6]) were mixed with 15.2 wt % binder at 178 °C for 10 min to form an anode paste, which were then formed as cylinders by pressing at 60 MPa. The CPC and CTP used in the work are materials currently used in the aluminium industry.

Twelve anodes were made at Laval University (6 CTP and 6 BP). Six anodes (3 CTP and 3 BP) were baked directly after pressing. The baking cycle consists of increasing the temperature to 150 °C (60 °C/h), then to 650 °C (20 °C/h), and finally to 1100 °C (50 °C/h), and this temperature was maintained for 20 h. Additionally, the six green anodes (3 CTP and 3 BP) were first investigated with µCT before one of each (BP-4 and CTP-4) was baked with a similar cycle at SINTEF Industry (almost a year after pressing). Despite the identical baking cycle settings, the major differences between the process at Laval and SINTEF are the size of crucible, height, packing density and type of packing coke, anode-anode distance in the crucible, and type and size of furnace. The size of the baking crucible used at SINTEF was 160 mm diameter and 150 mm height. The two anode samples were placed with approximately 30 mm distance between, and the crucible was then filled to the top by packing coke sized 0-5 mm.

2.2 µCT

Due to instrumental availability issues and time constraints, three different µCT labs with similar instruments had to be used in this work. They are all 225 kV tungsten reflection target instruments (cone beam volume CT) delivered by Nikon, but with different manipulator distances and panel sizes. The parameters were adjusted to give matching voxel sizes. Different scans were done at different scan volumes, to cover the samples at different sizes and resolution. The smaller volumes provide more details, but only cover the middle part of the sample in the height direction. The images were exported as 16-bit TIFF and processed in the public domain software ImageJ [8]

using scripts developed at SINTEF. A general description of the method is published elsewhere [9]. Table 1 shows the µCT scanning parameters applied in this work.

Table 1. Relevant µCT scanning parameters.

	µCT Laboratory		
	1*	**2****	**3*****
Scan width	55 mm	55 mm	113 mm
Figures	Figure 3-Figure 8 left	Figure 3-Figure 8 right	Figure 2, Figure 9
Acceleration voltage [kV]	150	150	150
Beam current [µA]	180	145	110
Filtering	none	none	none
Integration time [ms]	354	708	250
Signal amplification [dB]	18	18	18
Projections per 360º	6283	6283	8954
Source to sample distance [mm]	156.06	156.14	251.59
Source to detector distance [mm]	1124.80	1125.28	947.19
Resulting voxel size [µm]	27.75	27.75	39.84
1*: Pore Imaging Laboratory at SINTEF, Trondheim, Norway Detector Panel: Varex 1621 EHS: 2000x2000 pixels @ 200x200 µm (total 40 x 40cm^2)			
2*: X-ray Laboratory at Department of Physics, NTNU, Trondheim, Norway Detector Panel: Varex 1620 AN: 2000x2000 pixels @ 200x200 µm (total 40 x 40 cm^2)			
3*: PoreLab at Department of Geoscience and Petroleum, NTNU, Trondheim, Norway Detector Panel: Varex 4343 CT: 2850x2850 pixels @ 150x150 µm (total 43 x 43 cm^2)			

2.3 Data Processing

Besides the descriptions given in [9], this work includes calculation of the anode shrinkage from the µCT data. This was done using a modified version of the bUnwarpJ plugin for ImageJ [10]. This plugin calculates an elastic transform for a grid of points covering the image, using vector splines. The modifications done included exporting the transform vectors as a table, allowing a correlation of the coordinate shift in the X and Y directions. These correlation factors were then used as a measure of the horizontal and vertical dimension change (shrinkage). No changes were made to the fitting algorithm.

3. Results and Discussion

3.1 Anode Properties

The anodes were made at Laval university and shipped to Trondheim for the µCT investigations. All twelve anodes were first scanned together in a low resolution µCT-scan to investigate any potential large-scale variations in the anode structure. The overview scan showed the anode structure to be quite consistent across all samples. The CTP-4 and BP-4 samples were selected for the pre- and post-baking investigation in this work.

Table 2 shows the dimensions and weight before and after baking. BP-1, BP-2, BP-3, CTP-1, CTP-2 and CTP-3 were baked at Laval. Samples BP-4 and CTP-4 were baked at SINTEF with a baking cycle similar to the one used at Laval, close to a year after they were fabricated at Laval. The values in Table 2 corresponds to values measured at Laval (except the baked values for the two samples baked at SINTEF). Unfortunately, the crucible size and the amount of packing coke used were insufficient during the baking experiment conducted at SINTEF, so there was some

gas induced burn-off at the top of the BP-4 sample. Only the top 2-3 cm seemed to be affected. Figure 1 shows a picture of the samples after baking.

Table 2. Anode samples before and after baking; dimensions height (H), diameter (D) in cm, volume (V) in cm^3, weight (W) in grams and density (ρ) in g/cm^3.

	Green Anodes					Baked Anodes				
	H	**D**	**V**	**W**	**ρ**	**H**	**D**	**V**	**W**	**ρ**
BP-1	9.132	5.136	189.18	297.0	1.570	8.951	5.072	180.84	274.9	1.520
BP-2	9.146	5.137	189.59	298.4	1.574	8.952	5.063	180.25	275.3	1.527
BP-3	8.873	5.140	184.12	288.3	1.566	8.691	5.069	175.42	266.7	1.520
BP-4	9.152	5.138	189.76	298.8	1.575	9.00*	5.086	182.86	264.6	1.447
BP-5	8.347	5.135	172.88	272.8	1.578					
BP-6	9.403	5.130	194.36	303.7	1.563					
CTP-1	9.422	5.138	195.38	306.0	1.566	9.316	5.089	189.47	291.6	1.539
CTP-2	9.464	5.133	195.88	308.7	1.576	9.383	5.083	190.43	293.1	1.539
CTP-3	9.175	5.130	189.64	298.9	1.576	9.079	5.083	184.21	284.6	1.545
CTP-4	9.415	5.135	194.97	303.8	1.558	9.350	5.105	191.38	288.7	1.509
CTP-5	9.414	5.137	195.12	304.9	1.563					
CTP-6	9.488	5.138	196.75	306.1	1.556					

*The sample had airburn at the top, so the height is only given as an approximate value.

Figure 1. BP-4 (left) and CTP-4 (right) samples after baking at SINTEF.

The CTP-4 and BP-4 samples were scanned by µCT before baking at 50 mm scan width to provide maximum detail, and 110 mm scan height to provide an image of the sample at full height. After baking, the samples were scanned at matching resolution to allow a before- and after- baking comparison of the µCT data. Figure 2 shows the 110 mm height scans of the samples before and after baking. The gas burn at the top of BP-4 after baking is clearly visible. The data is oriented so that the images show the same position in the sample, allowing detail to be matched.

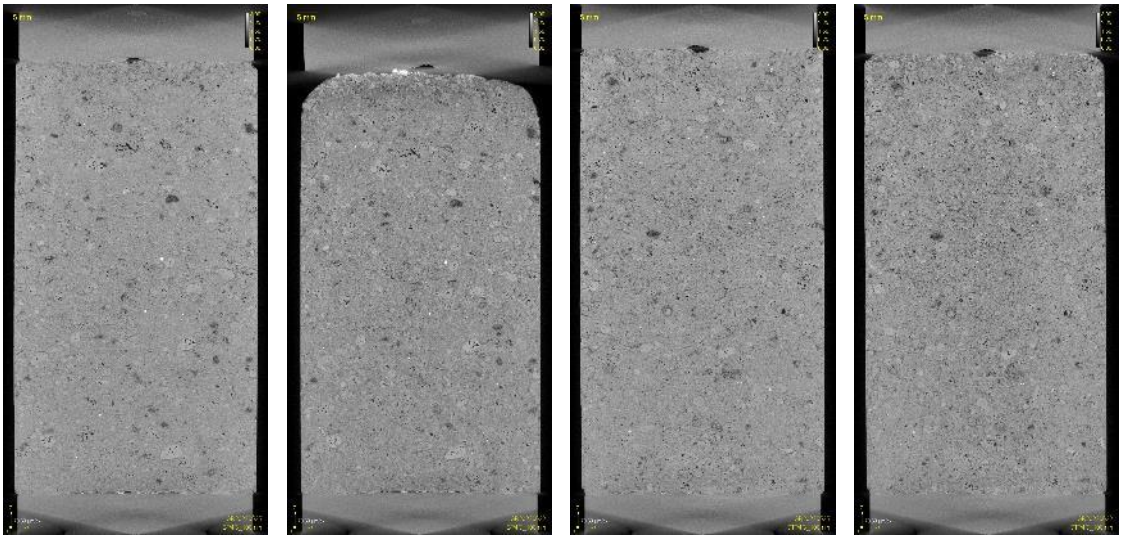

BP-4 green BP-4 baked CTP-4 green CTP-4 baked

Figure 2. 110 mm height scans of samples before and after baking.

3.2 Qualitative Observations in the µCT Data

Figure 3 shows 50 mm width scans of the BP-4 sample before and after baking, as horizontal cuts of the µCT data through the middle of the sample in the vertical direction. Since the details are hard to see at this scale, blue squares indicate the position of smaller 12x12 mm2 size crops, shown in Figure 4. The data is aligned to the same position in the sample ±100 µm, so the same grains and their placement in the binder phase can be seen for both the green and baked samples. Figure 5 shows 50 mm width scans of BP-4 sample before and after baking as a vertical cut, with the matching 12 mm x 12 mm vertical cut crops of the BP-4 sample in Figure 6.

The vertical cuts reveal some more detail of the anode structure; there is significant horizontal cracking, especially between the grains and binder phase. The coke grain mixture consists of both isotropic and anisotropic grains. The isotropic coke grains (characterized by a rounded shape) have a brighter shade of grey, meaning they attenuate more X-rays. (Calculations of X-ray attenuation [11] for this energy range show that carbon with 4 % S (by weight) has ~11 % higher X-ray attenuation than carbon with 1 % S). There is more cracking around these isotropic grains.

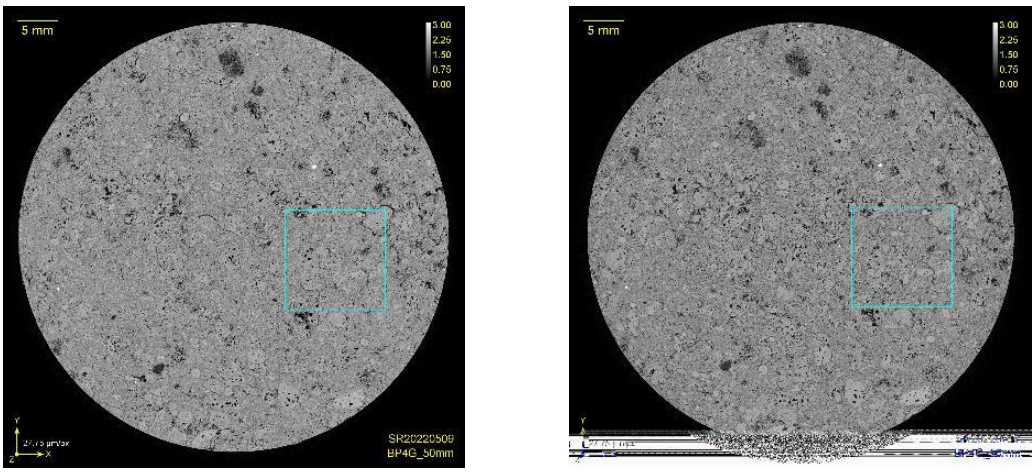

Figure 3. 50 mm width scan of BP-4 sample, green (left) and baked (right), horizontal cut.

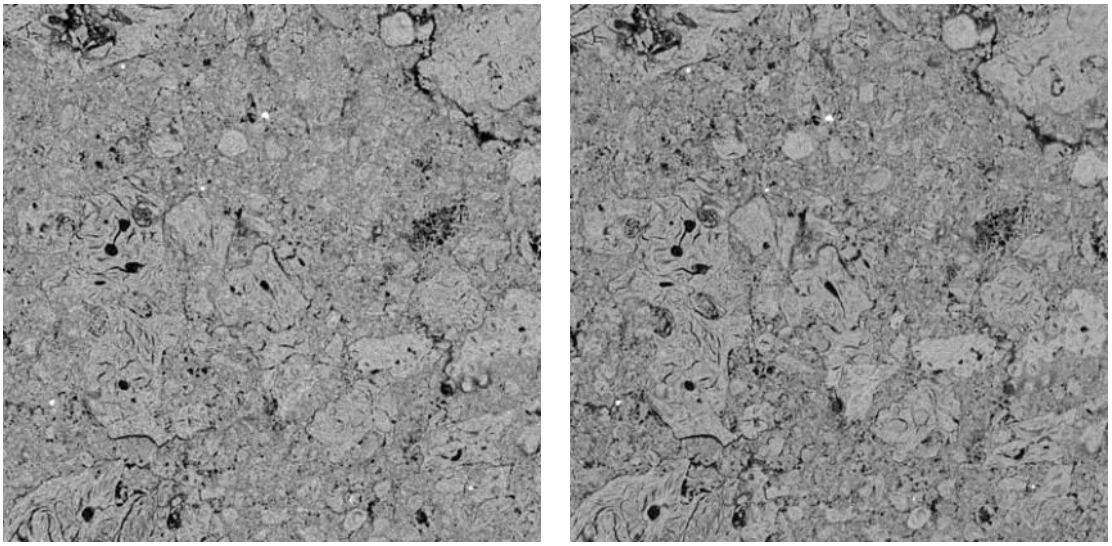

Figure 4. 12x12 mm^2 crop from BP-4 sample, green (left) and baked (right), horizontal cut.

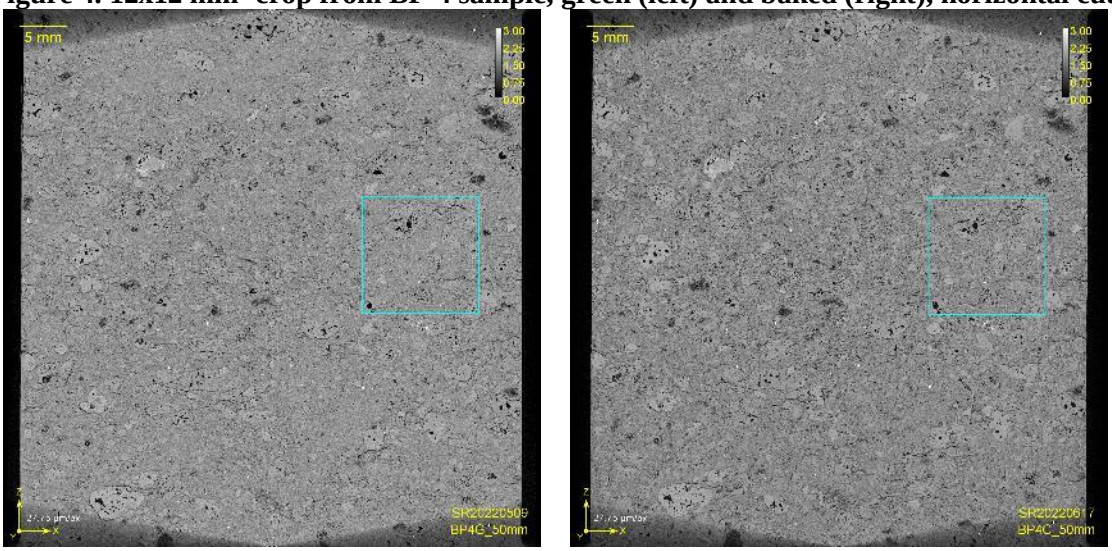

Figure 5. 50 mm width scan of BP-4 sample, green (left) and baked (right); vertical cut

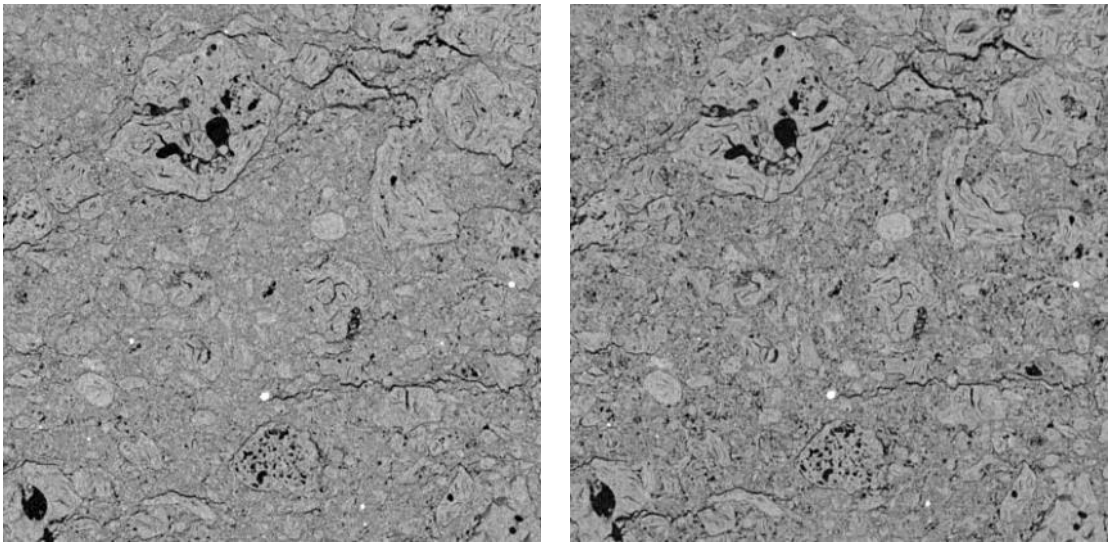

Figure 6. 12x12 mm^2 crop from BP-4 sample, green (left) and baked (right), vertical cut.

Figure 7 shows a 12x12 mm^2 crop from a 50 mm width scan of CTP-4 sample before and after baking, horizontal cuts. Figure 8 shows 12x12 mm^2 crop from a 50 mm width scan of CTP-4 sample before and after baking as vertical cuts. Comparing the green and baked anodes in Figure 6 and Figure 8, there seems to be some reduction in the degree of cracking after baking. There appear to be a higher reduction of cracking in the BP-4 sample, possibly due to the higher shrinkage of the bio-pitch after baking.

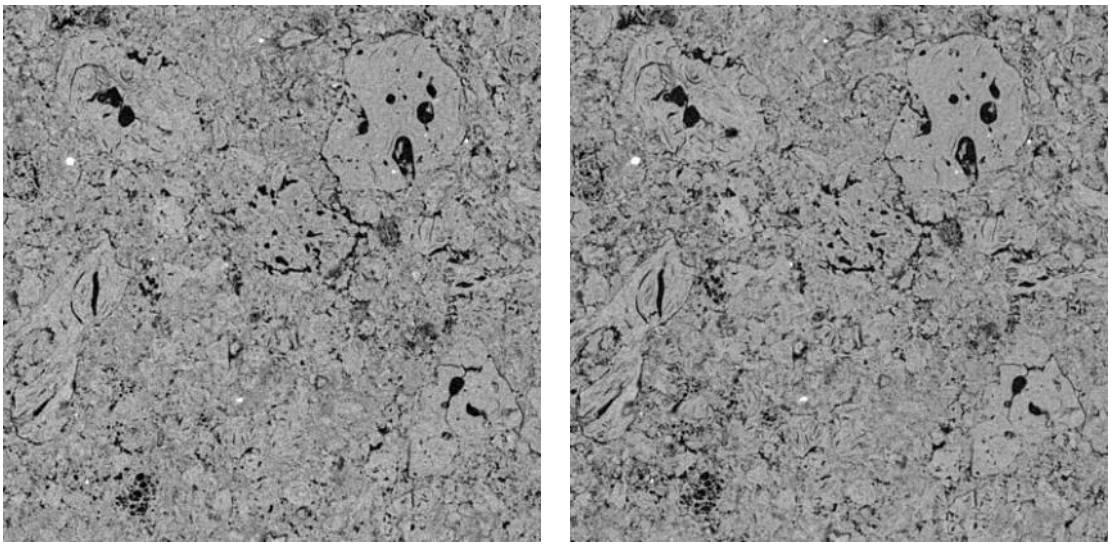

Figure 7. 12x12 mm2 crop from CTP-4 sample, green (left) and baked (right), horizontal cut.

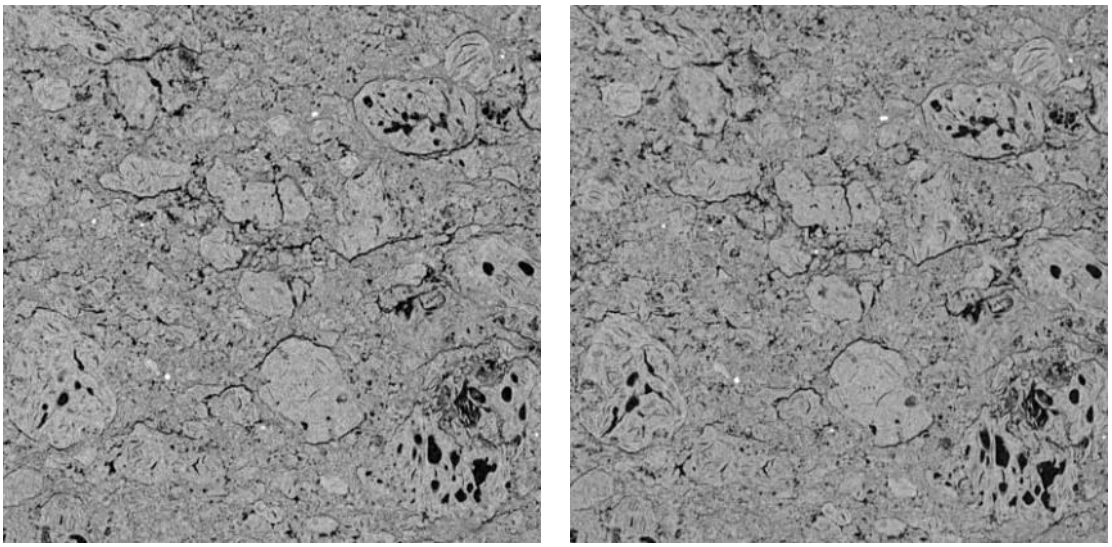

Figure 8. 12x12 mm2 crop from CTP-4 sample, green (left) and baked (right), vertical cut.

Overall, including the other anode samples baked at Laval University (not imaged), the BP samples have a similar structure as the CTP samples. The CTP samples show the same cracking around the isotropic coke grains as in the BP samples. The CTP samples also show the same tendency for horizontal delamination, as visible in the vertical scan images. For both the BP and CTP samples, there are more cracks near the cylindrical edge of the sample.

The baking loss of the binder phase can be seen as an overall darkening of the material between the grains. There are no obvious differences between the BP and CTP samples in the baking loss.

Figure 9 shows a 15x15 mm^2 crop from BP-4 sample, green (left) and baked (right). This is a vertical view of top edge corner, which shows the selective oxidation of binder phase. The coke grains retain their density, while the binder phase darkens due to the increase in small-scale porosity between the fine particles. This selective "gas-burn" of the binder shows that there is significant gas diffusion inside the sample.

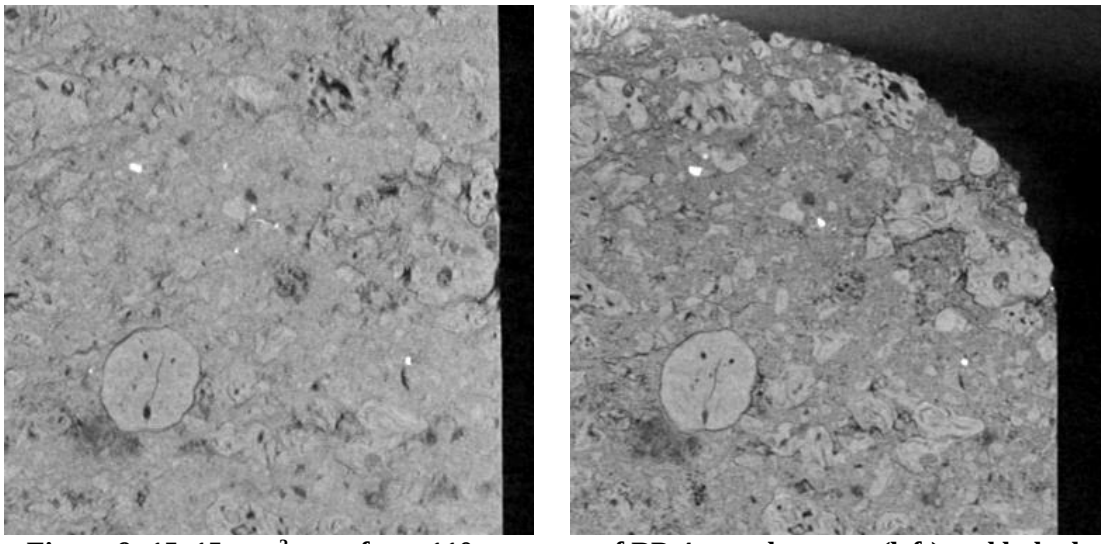

Figure 9: 15x15 mm^2 crop from 110 mm scan of BP-4 sample, green (left) and baked (right); vertical view of top edge corner, showing selective oxidation (gas-burn) of binder phase.

3.3 µCT Measurement of Density and Porosity

The µCT software calculates X-ray attenuation values for all points in the volume. These will depend both on the atomic number and the density of the material. Since the samples consist of mostly carbon, the calculated attenuation values will be more or less directly proportional to the geometric density of the material. Figure 10 shows a plot of the calculated density as a function of Z position for all samples. The X-ray attenuation values is higher for heavier elements than carbon. This is because the X-rays are attenuated by mostly interaction with the electrons at these energies, but the size of the electron cloud is proportional to the atomic weight by a factor less than 1. Because of this effect, a constant correction factor of 0.88 was calculated empirically and multiplied to all the density values. This factor reflects the degree the fraction of atoms in the sample with an atomic weight higher than carbon attenuates X-rays more than carbon, and is assumed to be the same for all samples. A theoretical calculation of this factor is possible, but complicated. It will require a complete elemental analysis of the sample, a correct model of the emitted polychromatic X-ray spectrum, a correct calculation of the scattering of the ambient air, and a correct plot of the spectral sensitivity of the panel. This is therefore outside the scope of this work, and not needed for comparison of the samples since all these factors are constant here.

The plots in Figure 10 show some transition in the shape of the profile below and above the middle of the sample. The reason for this is not known. The gas burn does not seem to affect the density below 70 mm, which is consistent with the visual appearance of the sample shown in Figure 1. The green density of the anode made with bio-pitch sample is higher than that of the anode made with CTP, while its baked density is lower. This was expected since the coking value of the BP is much lower than that of the CTP.

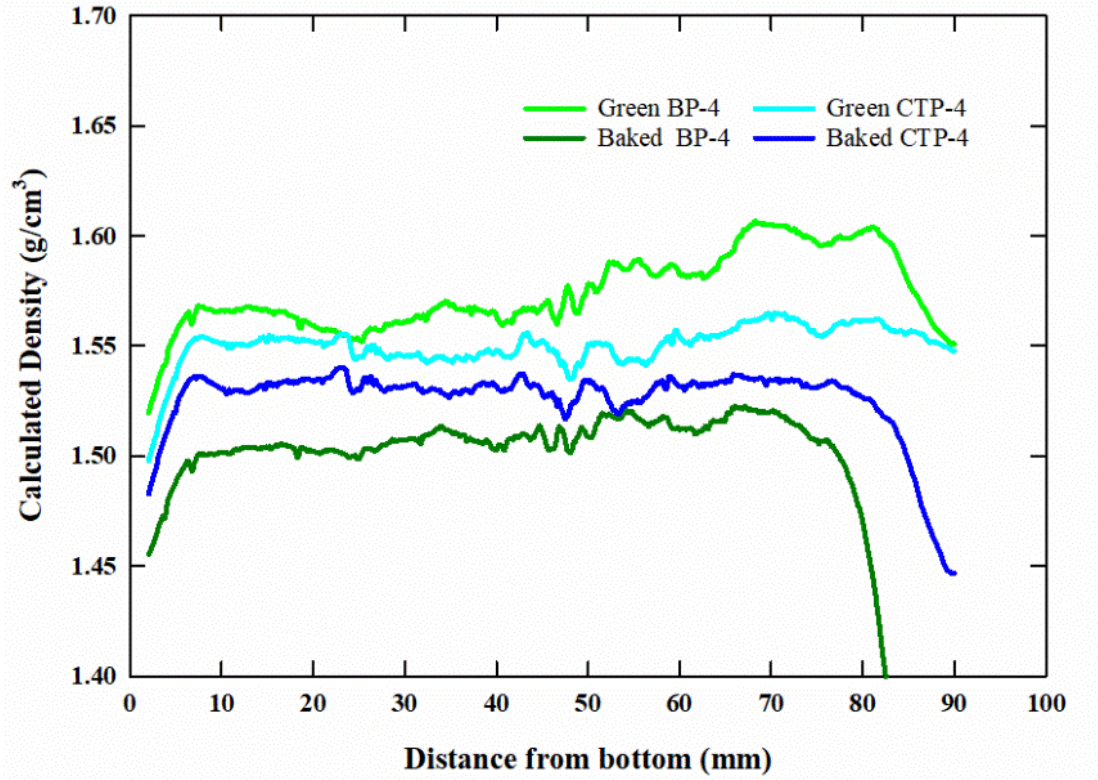

Figure 10. Plot of calculated density as a function of the distance from the bottom for BP-4 and CTP-4 samples in both green and baked states.

Pore size measurements were not done in this work. The resolution at 27 µm voxel size for the 50 mm samples is not sufficient to provide reliable values, as a significant fraction of the porosity is below this size. Also, it is not considered to be relevant for the overall macro structure of such samples, as the porosity is quite evenly distributed throughout the sample volume. Since the coke raw material is the same, the porosity difference between materials is sufficiently given by the density distribution reported in the previous section.

3.4 Measurement of Shrinkage

Table 3 shows coordinate correlation factors, as calculated from the µCT data using the bUnwarpJ plugin. These numbers indicate the correlation between the coordinates of the points in the baked anode matching the green anode. The slope is thus equal to the shrinkage, and the R2 correlation value is a measure of the uniformness of the shrinkage. The values for R2 are very close to 1.0, meaning that the shrinkage is uniform in each of the directions. There is a larger shrinkage in the vertical direction, which is not unexpected as the anode samples were pressed vertically during manufacturing.

Table 3. Coordinate correlation factors, as calculated from µCT data.

	BP-4		CTP-4	
	Horizontal	**Vertical**	**Horizontal**	**Vertical**
Slope	0.988881	0.984872	0.992641	0.990916
Correlation (R^2)	0.999990	0.999996	0.999986	0.999999
Shrinkage = (1-slope)*100 %	1.11 %	1.51 %	0.74 %	0.91 %

Table 4 shows the anode samples shrinkage, as measured by a mechanical calliper. The values calculated from the µCT data are repeated here. The calliper resolution is 0.05 mm, which

corresponds to 0.1 % of the 50 mm diameter of the anodes. This can be a reason for the small discrepancy between the calliper measurements and the ones calculated from the µCT data. The lower values for the calliper measurements compared to both the anodes baked and measured at Laval can also be explained by different people doing the measurements with different callipers. The calliper measurements done at SINTEF was up to 0.20 % higher for the anodes that arrived in the baked state. Taking this into consideration, the shrinkage of BP-4 and CTP-4 is still smaller than the anodes baked at Laval, but the discrepancy may be lower than Table 4 indicates.

Table 4. Anode samples shrinkage, as measured by calliper and calculated from µCT data.

	Horizontal shrinkage		Vertical shrinkage	
	Calliper	**µCT**	**Calliper**	**µCT**
BP-1	1.25 %		1.98 %	
BP-2	1.44 %		2.12 %	
BP-3	1.38 %		2.05 %	
BP-4	1.01 %	1.11 %	1.66 %*	1.51 %
CTP-1	0.96 %		1.13 %	
CTP-2	0.98 %		0.85 %	
CTP-3	0.92 %		1.05 %	
CTP-4	0.58 %	0.74 %	0.69 %	0.91 %

* The sample had gasburn at the top, so the calliper height results in an approximate value.

Long storage time between forming and baking for the anodes baked at SINTEF might have resulted in shrinkage in the green state, however the shrinkage for these samples is still lower that the ones baked directly after forming. The remaining green samples were evaluated for such behaviour, and no shrinkage was observed compared to the values measured directly after forming.

4. Further Evaluations on Anode Quality

There are two likely explanations to the observed higher degree of cracking around the isotropic/high sulfur grains:

1) There is poorer wetting between the binder phase and the isotropic grains than the anisotropic grains.
2) The isotropic grains are less flexible, and will thus absorb less energy during the pressing of the anodes. They will then detach more easily from the binder phase when the pressure is released.

Since both the BP and CTP anodes show this cracking around grains, and vibrated anodes investigated in other work [9] do not show such cracking, the hypothesis (2) is considered a more likely explanation than (1).

In future work, it would be of interest to examine the wetting between bio-pitch and high-sulfur coke by measuring the wetting angle between pitch and a coke bed (like in [5]) and compare these results to a low-sulfur anisotropic coke.

Anodes made from BP and CTP have previously been shown to have similar physical [6] and electrochemical [7] properties when made by this method. Observations in this work indicate that both BP and CTP anodes made in this facility have cracking around the isotropic grains, which again may influence the anode properties more than the type of binder used. For this reason, it would be of interest to make anodes from bio-pitch in a pilot scale vibro-forming facility, to see if this eliminates the observed cracking around grains, and if the BP and CTP anodes keep their similarities or new differences is observed.

Since the anode density is in the lower end of what is common for industrial anodes, the effect of higher binder levels could be investigated in future work. There is usually a trade-off between higher binder level and higher permeability, as too much binder will cause the anode to expand during baking. Since the baking loss is higher for bio-pitch, the optimum binder level value can be higher for bio-pitch than for coal tar pitch.

Obviously, the density of the packing coke bed must be improved to avoid gas-burn, compared to what was done in this single baking experiment at SINTEF. Time and budget constrain did not allow for a second baking experiment.

It is possible to get a higher resolution scan of the full anode sample height using helical scanning mode, which is available in the new Pore Imaging Laboratory. This was not attempted in this work, as it requires some further optimization of scanning parameters beyond what has been done in our initial testing. Helical scanning is challenging with carbon materials due to their low attenuation contrast.

5. Conclusions

In this work, pilot anodes made with coal tar pitch and bio-pitch were investigated by μCT before and after baking. The resulting images are of high quality, demonstrating the method's usefulness when wanting to investigate the internal structure of anodes in a non-destructive way. In fact, images from the entire anode can be extracted from the dataset. Cracks are observed for both types of anodes in the vicinity of the isotropic/high sulfur grains, although a reduction of this cracking is observed after baking (more so for the BP anodes than the CTP anodes). It is suggested that the reason for the observed cracks is caused by the low flexibility of these types of coke grains, in combination with the method used to produce the anodes (pressing). Otherwise, baking gives only a small change to anode structure (loss of binder), and no significant macro-scale effects are visible. Overall, our μCT-based investigation suggests that the anode samples made of CTP and Bio-pitch have very similar microstructures, which agrees with their similar physical and electrochemical properties reported earlier.

Acknowledgements

This research was funded by Research Council of Norway grant number 294679 (BioCarbUp).
The authors would like to acknowledge the use of the Pore Imaging Laboratory (NO3.7d) at SINTEF Industry; research infrastructure under ECCSEL ERIC (The European Research Infrastructure for CO2 Capture, Utilisation, Transport and Storage). The Research Council of Norway is acknowledged for the support to the CT scan facilities of the Center of Excellence PoreLab, project number 262644; at the Department of Geoscience and Petroleum, NTNU, Trondheim, Norway. The authors would also like to acknowledge the use of the laboratory of the X-ray Physics Group at NTNU, part of the National Infrastructure NEXT, funded by NTNU, the Norwegian Research Council, and European program INFRAIA (90659800).

6. References

1. Belkacem Amara et al., Modification of biocoke destined for the fabrication of anodes used in primary aluminum production, *Fuel*, Vol. 304, 121352.
2. Belkacem Amara et al., Effect of Coke Type on Partial Replacement of Coke with Modified Biocoke in Anodes Used in Primary Aluminum Production, *Light Metals* 2022, 818-825.
3. Camilla Sommerseth et al., Charcoal and Use of Green Binder for Use in Carbon Anodes in the Aluminium Industry, *Light Metals* 2020, 1388-1347.

4. J.D. Rocha, A.R. Coutinho, and C.A. Luengo, Biopitch produced from eucalyptus wood pyrolysis liquids as a renewable binder for carbon electrode manufacture, *Brazilian Journal of Chemical Engineering*, Vol. 19, (2002), 127-132.
5. Ying Lu et al., Properties of Bio-pitch and Its Wettability on Coke, *ACS Sustainable Chemistry & Engineering*, Vol. 8, No. 40, (2020), 15366-15374.
6. Asem Hussein, Donald Picard, and Houshang Alamdari, Biopitch as a Binder for Carbon Anodes: Impact on Carbon Anode Properties, *ACS Sustainable Chemistry & Engineering*, Vol. 9, No. 12, (2021), 4681-4687.
7. Asem Hussein et al., Electrochemical Performance of Carbon Anodes Made of Bio-pitch as a Binder, Metallurgical and Materials Transactions B, Vol. 53, No. 1, (2022), 584-593.
8. W.S. Rasband, Image J and U. S. National Institutes of Health, Image processing and analysis in Java, http://imagej.nih.gov/ij/
9. Stein Rørvik and Lorentz Petter Lossius, Characterization of Prebake Anodes by Micro X-ray Computed Tomography, *Light Metals* 2017, 1237-1245
10. I. Arganda-Carreras et al., Consistent and Elastic Registration of Histological Sections using Vector-Spline Regularization, *Lecture Notes in Computer Science: Computer Vision Approaches to Medical Image Analysis*, Vol. 4241, (2006), 85-95.
11. X-Ray Form Factor, Attenuation, and Scattering Tables *(NIST Standard Reference Database* 66) https://www.nist.gov/pml/x-ray-form-factor-attenuation-and-scattering-tables (calculator at https://physics.nist.gov/PhysRefData/FFast/html/form.html)